Triton's streaks as windblown dust

Carl Sagan & Christopher Chyba

Laboratory for Planetary Studies, Cornell University, Ithaca, New York 14853, USA

THE encounter of the Voyager 2 spacecraft with Neptune's satellite Triton revealed many 'dark' (about 10–20% darker than the adjacent frost) surface streaks in Triton's southern hemisphere[1], resembling the streaks that are due to windblown dust on Mars[2]. It seems therefore that dust transport by winds in Triton's tenuous atmosphere is required, the main question being the mechanism for raising dust from the surface or sub-surface. The two obvious candidates are geyser-like eruptions and direct lofting by surface winds[1]. Here we show that, despite Triton's tenuous (16 ± 3 μbar) atmosphere[3], low-cohesion grains with diameters of $\lesssim 5$ μm, may be carried into suspension by aeolian surface shear stress, given expected geostrophic wind speeds[4] of ~ 10 m s^{-1}. (The wind velocities needed to lift grains as cohesive as those found on Earth, however, are implausibly high.) For erupting plumes, we show that dust-settling timescales and expected wind velocities yield streak length scales in good agreement with those observed. Both candidate mechanisms therefore seem to be consistent with present observations of Triton.

Ground-based observations of seasonal and secular albedo changes on Mars were explained by Sagan and Pollack[5,6] in terms of windblown dust. Based on the classic study by Bagnold[7], they showed that the threshold critical velocity to initiate grain motion at the base of the martian boundary layer is consistent with plausible wind velocities on Mars. (We call all such transport—whether the particles maintain their ballistic trajectories or are entrained by winds—saltation, from the Latin word for 'jump'.) Subsequent Mariner 9 and Viking data revealed time-variable dark irregular 'splotches', and bright and dark 'streaks' typically tens of kilometres long, many emanating from impact craters[2,8,9]. Martian general circulation and topographic slope winds generally seem strong enough, and in the proper directions, to account for the wind streaks[2,9].

The dependence of threshold friction velocity (the minimum wind speed required for saltation) on particle diameter D_p is usually taken to be roughly parabolic[7]. The velocity increases to large D_p because drag scales as the area but the mass scales as the volume. At lower diameters, the increase of threshold velocity with decreasing D_p was also thought, from limited data, to be a fluid mechanics effect[7]. But subsequent work[10-14]—including data on cohesion-free particle transport in fluid beds—indicates that the effect is due to cohesion, which increases the effective weight of small grains.

Although the surface pressure on Triton is only ~0.25% that on Mars, dark streaks of a remarkably martian aspect are observed on Triton's southern summer polar cap. Like many martian streaks, those on Triton are mainly tens of kilometres long. Although association with impact craters, rare in the Triton polar cap, is not generally evident, Triton streaks frequently emanate from dark splotches a few kilometres across (and, more rarely, from small bright regions)[1].

The mass loading of Triton's atmosphere is $P/g \approx 0.2$ g cm^{-2} (where $P = 16 \pm 3$ μbar nitrogen and $g = 78$ cm s^{-2} are Triton's surface pressure[3] and gravitational acceleration, respectively), and the amount of ice (presumably nitrogen and methane) deposited on the polar cap in winter is probably more than enough to cover over any preexisting streaks. Such streaks might be exposed again in the following spring and summer, but it is also possible that new streaks are produced in the caps once each seasonal cycle (~165 Earth years long).

A plausible source of the (relatively) dark material on Triton is complex organic heteropolymers produced by neptunian magnetospheric electrons, cosmic rays and solar ultraviolet radiation[15]. These organics might be formed in the atmosphere, or directly on the surface from methane and other hydrocarbon ices[15,16]. An origin from processes inside Triton, such as ice volcanoes or fumaroles, is also possible[1]. This would readily explain the association of streaks with particular small source regions; particles could then be transported either in suspension by the prevailing winds at altitude, or by saltation and subsequent entrainment by winds nearer the surface. A rosette diagram of the directions of wind streaks on Triton[17] shows preferred orientations approximately consistent with those given by Ingersoll's[4] general circulation model. If the dark material is generated by radiation in the atmosphere, its arrival at the surface in small particles would be easily understood, but its concentration in source regions would require preferential trapping in topographic features below the resolution limit, as is thought to occur on Mars (in crater floors, for example[2,8]).

The threshold wind velocity u_{*0} to initiate motion of particles of diameter D_p and density ρ_p where the atmospheric density is ρ is given by[7]

$$u_{*0} = A(D_p g \rho_p / \rho)^{1/2} \tag{1}$$

where the Bagnold parameter A is a dimensionless constant that is a measure of the ratio of the mean fluid shear stress to the gravity stress on the topmost layer of dust grains; typically, $A \approx 0.1$. Equation (1) can be derived within the factor A by equating the gravitational force mg on a particle of mass m to the dynamic wind pressure ρu_*^2 acting on the cross-sectional area of the particle. Traditionally[7], A has been taken to be a function only of B, the frictional Reynolds number, $B = D_p u_{*0}/\nu$, where ν is the kinematic viscosity. But fluid-bed and wind-tunnel experiments show that for small particles with $B \leq 1$, A is a function not only of B, but also of interparticle forces[10-14].

Surface gravity and atmospheric pressure on Triton are in good agreement with an assumption of vapour-pressure equilibrium at a surface temperature[18] of 38^{+3}_{-4} K. From the ideal-gas law, $\rho = 1.4 \times 10^{-7}$ g cm^{-3}. Mars has $g = 371$ cm s^{-2} and $P \approx 6$ mbar CO_2, giving $\rho = 1.5 \times 10^{-5}$ g cm^{-3} for a surface temperature[19] of 215 K. Dust densities on Mars are probably those appropriate to sand[7,11], ~2.7 g cm^{-3}. Dust on Triton is probably a combination of methane or nitrogen ice and dark organics[1]. Densities for methane and nitrogen ices are 0.5 g cm^{-3} and 0.9 or 1.0 g cm^{-3}, respectively[20], with the latter density determined by whether nitrogen is present in its α or β form [the α-β phase transition occurs at 35.6 K (ref. 21 and R. H. Brown, personal communication)]. Typical densities for condensed simple organics are ~0.5–0.7 g cm^{-3}, and for more complex organics[22] are 0.7–1.2 g cm^{-3}. We take $\rho_p = 0.75$ g cm^{-3} as a typical dust density on Triton.

The ratio of the threshold wind velocity for particle motion on Triton to that on Mars is then, from equation (1),

$$u^T_{*0}/u^M_{*0} = 2.5(A^T/A^M)(D^T_p/D^M_p)^{1/2} \tag{2}$$

where the superscripts T and M refer to Triton and Mars. Equation (2) shows that for particles of a given diameter, the threshold wind velocity on Triton is only ~2.5 times higher than that on Mars, assuming that the value of the Bagnold parameter is the same.

Given the extremely low atmospheric pressures of Triton ($P^M/P^T \approx 400$), these results seem counterintuitive; but there are four factors that mitigate the effect of low pressure: Triton's surface gravity is lower than that of Mars by a factor of ~5, dust densities on Triton are probably lower by a factor of ~3, u_{*0} depends on the density, not the pressure, ratio (atmospheric density depends inversely as temperature, and Triton's temperature is a factor of ~6 lower than that of Mars), and u_{*0} has only a square-root dependence on all of these parameters.

What is u_{*0} for Triton? First we must determine B. Ingersoll[4] has used scaling arguments to obtain a kinematic viscosity $\nu = 450\ \mathrm{cm^2\ s^{-1}}$. Given this value, even particles with D_p as large as 0.1 cm will have $B \ll 1$ for any plausible u_{*0} (see below), so that we are in the highly laminar regime where A depends on both B and D_p. Iversen *et al.*[11] fit an analytical model for u_{*0} incorporating drag and lift, rotational moment of inertia, weight and interparticle forces to a variety of wind-tunnel data, including experiments in the regime of very low air density and Reynolds number. These latter experiments were greatly extended by Iversen and White[13]. Greeley and Iversen[14] fit these data, for $B \leq 0.3$, with an expression like equation (1), but with the coefficient A given by

$$A \equiv A(B, D_p) = 0.2[(1 + I_p/\rho_p g D_p^3)/(1 + 2.5B)]^{1/2} \qquad (3)$$

where the interparticle force I_p is found to be $0.006 D_p^{1/2}$. From equations (3) and (1), we determine u_{*0} as a function of D_p, for the case where Triton dust is subject to interparticle forces (cohesion) comparable to those between terrestrial grains.

We also consider the possibility that interparticle cohesion on Triton is much weaker than on Earth (or on Mars, or on the Moon). Cohesion owing to thin adsorbed layers of liquid water, important on Earth[13,23,24], is certainly missing on Triton. The cohesion of lunar grains is greater than that of terrestrial grains[25], partly owing to agglutination from micrometeorite impacts[26] and partly to vacuum sintering[14]. Both effects may be weakened in the thin atmosphere of Triton. There is some (weak) spectroscopic evidence for water ice at Triton's surface[27], in which case hydrogen bonding might act as an interparticle cohesive force. In the absence of significant surficial water ice, perhaps only van der Waals forces[28] remain effective. We therefore analyse the two extremes—one in which cohesion is comparable to that of Earth, and the other in which there is no cohesion at all.

A number of investigators have considered the cohesionless regime[10-14], and it has been invoked to avoid having to postulate Mach 0.5 winds on the slopes of Pavonis Mons on Mars[29]. In this case, u_{*0} is given by equations (1) and (3) with I_p set equal to zero. In Fig. 1, we show aeolian threshold frictional velocities for particle motion on Triton for both cohesive and cohesionless grains, as a function of D_p. For cohesive grains, threshold velocities of at least $\sim 10\ \mathrm{m\ s^{-1}}$ are required for particle motion. In the cohesionless case, however, velocities as low as ~0.4–1.0 m s^{-1} will be sufficient to loft ~1–10 μm grains.

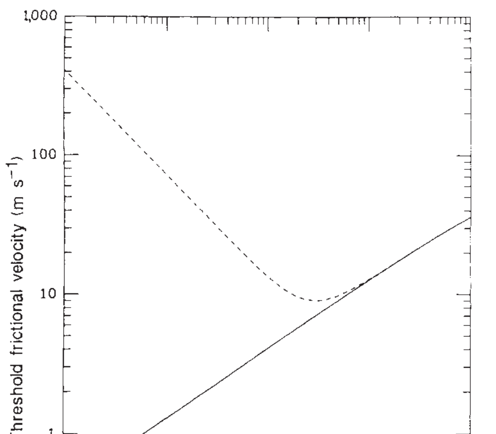

FIG. 1 Threshold velocity as a function of particle radius for cohesive (dashed line) and cohesionless (solid line) dust particles on Triton.

Can friction velocities u_* of this magnitude occur at Triton's surface? Ingersoll[4] has studied the dynamics of Triton's atmosphere, and finds wind speeds v at the top of a ~1-km boundary layer to be of the order of Triton's tangential speed of rotation, 16.7 m s^{-1}. The friction velocity should be related to v according to $v^2/u_*^2 = 1/C_D$, where the drag coefficient $C_D \approx 0.002$ (ref. 4). This approach gives $u_* \approx 0.75\ \mathrm{m\ s^{-1}}$.

A second approach, given v at the top of the boundary layer, is to adopt the standard Prandtl logarithmic variation of wind velocity with distance z above the surface[14,24]

$$v = (u_*/k)\ln(z/z_0) \qquad (4)$$

where $k = 0.4$ is the von Kármán constant and z_0 is the roughness length, a function of both Reynolds number and the shape of and distance between surface-roughness elements; typical prescriptions for z_0 range from $D_p/30$ for rough surfaces[14] to $\nu/30u_*$ for small B (ref. 12). Because of the logarithmic dependence in equation (4), u_* is insensitive to z_0. Taking z to be the height of the boundary layer[4] (~1 km), equation (4) with the above choices of z_0 gives $u_* \approx 0.3$–$0.4\ \mathrm{m\ s^{-1}}$, in rough agreement with the calculation based on C_D. Thus, surface friction velocities $u_* \approx 0.1$–$1.0\ \mathrm{m\ s^{-1}}$ seem probable. Figure 1 therefore shows that saltation is possible for cohesionless grains with diameters $D_p \leq 5\ \mu m$. If $z_0 \gg 5\ \mu m$, however, such grains might typically lie entirely within the laminar sub-layer below z_0, within which wind velocities could be much less than u_* (ref. 14). The required threshold wind velocities for cohesive grains are an order of magnitude too high. Unless wind gusts within ~100 μm of the surface occasionally reach ~10 m s^{-1}, about the value at the top of the boundary layer, grains as cohesive as silicate particles on Earth cannot be set into motion by Triton's winds. A possible exception would be entrainment initiated by bombardment of grains on Triton's surface by dust falling from erupted plumes. On Earth, such impact-induced entrainment can maintain movement of cohesive grains for wind velocities at or below those sufficient for initiating movement of cohesionless grains[7,14,24].

Finally, we compare u_* with the terminal velocity V(derived in equation (5) below) of a settling particle. Evidently $V < u_*$ for any value of u_* capable of lifting a particle of diameter D_p. This implies that any grain lofted from Triton's surface would be placed into suspension, rather than moving in low, multiple hops, which occurs only when $V \geq u_*$ (ref. 14).

Another potential mechanism for producing streaks is geyser-like eruptions[1] which inject dust into the prevailing winds (possibly analogous to the formation of elongate albedo markings on Io[30]). The fact that the surface streaks observed between 10° and 30° S trend towards the northeast implies that they are controlled by winds in the boundary layer, that is, within ~1 km of the surface[4]. This, then, will be our choice of injection height h for calculating the effects of wind velocities and fallout timescales for injected dust. Poleward of 30° S, however, streak directions become more irregular[1]. Similar dark streaks with diffuse downwind boundaries will be produced by settling dust whether it is geysered or saltated up into suspension.

Dust settling may occur in the Stokes (viscous) regime, when the gas mean free path $\lambda \ll D_p$, or in the Epstein (kinetic) regime, when $\lambda \gg D_p$. The mean free path is $(\sqrt{2}n\sigma)^{-1}$, where n is the number density and σ the collison cross-section of the gas. For Triton's nitrogen atmosphere, $n = 3.1 \times 10^{15}\ \mathrm{cm^{-3}}$, and $\sigma = 4.3 \times 10^{-15}\ \mathrm{cm^2}$ (ref. 31), giving $\lambda = 530\ \mu m\ (16\ \mu bar/P)$. Thus, settling dust on Triton is in the Epstein regime when $D_p \leq 100\ \mu m$. Settling speed V in the Epstein regime may be calculated by equating the gravitational force on a dust particle, mg, to the buoyancy force F exerted by the atmosphere, assuming no convective transport. For a spherical dust particle, $F = (\pi/3)\delta\bar{v}\rho D_p^2 V$, where $\bar{v}$ is the mean molecular speed, and δ is a constant that depends on the law of reflection of gas molecules from the surface of a sphere[32,33]. For specular reflection, $\delta = 1.0$, and for diffuse reflection $\delta = 1.4$. As the latter value is in good agreement with experiment[32,33], we adopt it here. Equating F

and mg yields $V=0.36D_p\rho_p g/\rho\bar{v}$, which for 10-μm particles becomes

$$V=8.9(D_p/10\ \mu\mathrm{m})(16\ \mu\mathrm{bar}/P)\quad \mathrm{cm\ s^{-1}} \qquad (5)$$

Thus a 10-μm particle will settle out from an injection height $h=1$ km in ~3 h.

The length of the dark streaks on Triton range from several tens to about one hundred kilometres[1]. Taking a characteristic length $L=50$ km, we find the required wind velocity in the boundary layer to be

$$v=L(h/V)=(L/50\ \mathrm{km})(1\ \mathrm{km}/h)(D_p/10\ \mu\mathrm{m})\ 4.5\ \mathrm{m\ s^{-1}}$$

Ingersoll[4] estimates typical wind velocities in the boundary layer to be ~$10\ \mathrm{m\ s^{-1}}$. Settling timescales and expected wind velocities in the boundary layer therefore yield streak length scales in good agreement with those observed. Larger particles will fall out closer to the source regions and smaller particles farther. Impacts by dust settling from such eruptions could then also initiate motion of surface grains.

If geysers or fumaroles loft significant amounts of dark dust in the boundary layer, it seems that the streaks can be well understood without any further hypotheses. This would, however, require a large number of geysers to have erupted, perhaps on as short a timescale as the ~165-yr seasonal cycle. The discovery[1] of two or three such eruptions during Voyager 2's few-hour flyby of Triton suggests that this is not a very stringent condition. Indeed, for hundreds of streaks to form on Triton over ~165 yr, on average several must erupt in any given year. The Voyager results then suggest that a typical geyser erupts for ~1 yr out of every 100, although these eruptions need not be continuous. (Moreover, we do not know whether Voyager's observation of two or three erupting plumes was typical of Triton, nor did Voyager image all of Triton's surface.) Consider a large dark streak, formed by such an eruption, ~100 km long and 10 km wide. A bright ice surface will be significantly darkened by an admixture of as little as 0.1–1.0% of dark dust[34]. Therefore ~1–10 $\mathrm{km^2}$ of dark dust is required to form the streak. For an average particle radius ~1 μm, this corresponds to ~10^5–10^6 g of dust. Thus to form a large dark streak, an eruption rate of dark dust as low as ~0.01–0.1 $\mathrm{g\ s^{-1}}$ for the 1-yr eruption period is required. A question for future research is whether geysers and saltation generate streaks with distinguishable characteristics. □

Received 14 March; accepted 18 June 1990.

1. Smith, B. A. *et al. Science* **246,** 1422–1449 (1989).
2. Sagan, C. *et al. Icarus* **17,** 346–372 (1972).
3. Tyler, G. L. *et al. Science* **246,** 1466–1472 (1989).
4. Ingersoll, A. P. *Nature* **344,** 315–317 (1990).
5. Sagan, C. & Pollack, J. B. *Smithson. astrophys. Obs. Spec. Rep. 255* (1967).
6. Sagan, C. & Pollack, J. B. *Nature* **223,** 791–794 (1969).
7. Bagnold, R. A. *The Physics of Blown Sand and Desert Dunes* (Chapman & Hall, London, 1954).
8. Sagan, C. *et al. J. geophys. Res.* **78,** 4163–4196 (1973).
9. Thomas, P., Veverka, J., Lee, S. & Bloom, A. *Icarus* **45,** 124–153 (1981).
10. Sagan, C. & Bagnold, R. A. *Icarus* **26,** 209–218 (1975).
11. Iversen, J. D., Pollack, J. B., Greeley, R. & White, B. R. *Icarus* **29,** 381–393 (1976).
12. Pollack, J. B., Haberle, R., Greeley, R. & Iversen, J. *Icarus* **29,** 395–417 (1976).
13. Iversen, J. D. & White, B. R. *Sedimentology* **29,** 111–119 (1982).
14. Greeley, R. & Iversen, J. D. *Wind as a Geological Process* (Cambridge University Press, 1985).
15. Thompson, W. R., Murray, B., Khare, B. N. & Sagan, C. *J. geophys. Res.* **92,** 14933–14947 (1987).
16. Khare, B. N. *et al. Icarus* **79,** 350–361 (1989).
17. Hansen, C. *et al. Geophys. Res. Lett.* (submitted).
18. Conrath, B. *et al. Science* **246,** 1454–1458 (1989).
19. Carr, M. H. *The Surface of Mars* (Yale University Press, 1981).
20. Simonelli, D. P. *et al. Icarus* **82,** 1–35 (1989).
21. Prokhavatilov, A. I. & Yantsevich, L. D. *Soviet J. low-temp. Phys.* **9,** 94–97 (1983).
22. Sagan, C., Thompson, W. R. & Khare, B. N. in *The Search for Extraterrestrial Life* (ed. Papagiannis, M. D.) 107–121 (Reidel, Boston, 1985).
23. Gregg, S. J. *The Surface Chemistry of Solids* Ch. 3 (Chapman & Hall, London, 1961).
24. Pye, K. *Aeolian Dust and Dust Deposits* Ch. 3 (Academic, London, 1987).
25. Mitchell, J. *et al. Proc. Third Lunar Sci. Conf.* Vol. 3 (ed. Criswell, D. R.) 3235–3253 (MIT Press, Cambridge, 1972).
26. Lindsay, J. F. *Lunar Stratigraphy and Sedimentology* Ch. 6 (Elsevier Scientific, New York, 1976).
27. Cruikshank, D. P., Brown, R. H. & Clark, R. N. *Icarus* **58,** 293–305 (1984).
28. Kitchener, J. A. in *Powders in Industry* 405–410 (Soc. chem. Ind., London, 1961).
29. Sagan, C. *et al. Icarus* **22,** 24–47 (1974).
30. Lee, S. W. & Thomas, P. C. *Icarus* **44,** 280–290 (1980).
31. Atkins, P. W. *Physical Chemistry* (Freeman, New York, 1986).
32. Epstein, P. S. *Phys. Rev.* **23,** 710–733 (1924).
33. Kennard, E. H. *Kinetic Theory of Gases* (McGraw-Hill, New York, 1938).
34. Clark, R. *Icarus* **49,** 244–257 (1982).

ACKNOWLEDGEMENTS. We thank R. H. Brown, P. Gierasch, C. Hansen, A. Ingersoll, T. V. Johnson, J. B. Pollack, J. Schwartz, L. Soderblom, P. C. Thomas and W. R. Thompson for discussions and suggestions. This work was supported by NASA.

Anomalous H^+ and D^+ conductance in H_2O–D_2O mixtures

H. Weingärtner* & C. A. Chatzidimitriou-Dreismann†‡

* Institut für Physikalische Chemie und Elektrochemie, Universität Karlsruhe, Kaiserstrasse 12, D-7500 Karlsruhe, FRG

† I. N. Stranski-Institut für Physikalische und Theoretische Chemie, Technische Universität Berlin, Strasse des 17 Juni 112, D-1000 Berlin 12, FRG

A KNOWLEDGE of proton-transfer dynamics and hydrogen-bonding in water and aqueous solutions is necessary for the understanding of many important chemical and biological processes. For example, quantum effects related to proton transfer (or tunnelling) in $H^+(H_2O)_n$ clusters of liquid water (where $n=1,2,\ldots$) are known to have a dominant role in the proton conductance mechanism[1,2] and are responsible for the high conductances of H^+ and OH^- in water. A new quantum theoretical approach to this process has been presented[3], which is based on the hypothesis that there are quantum correlations[4–8] between each H^+ and the protons of the surrounding water molecules, leading to the formation of coherent dissipative structures[3,8]. From further investigations, one of us predicted that an anomalous decrease of H^+ conductance in H_2O–D_2O mixtures would take place[9]. Having thought of an experiment to test these predictions[9] we now report the experimental results and conclude that an anomalous decrease in proton conductance does indeed occur.

The aforementioned experiment consists in the measurement of molar conductances of different HCl-DCl and KCl solutions in H_2O-D_2O mixtures. The experimental set-up, the results and their analysis are as follows.

For solutions in normal water, we used deionized and distilled H_2O with a specific conductance of ~$1\times10^{-6}\ \mathrm{S\ cm^{-1}}$. A stock solution of HCl in H_2O with a molar concentration of $\geqslant 0.5\ \mathrm{mol\ dm^{-3}}$ was prepared, the exact concentration of which was determined by potentiometric titration of H^+ against NaOH and of Cl^- against $AgNO_3$. The concentration of this solution was then adjusted to $0.5\ \mathrm{mol\ dm^{-3}}$ (error $<\pm0.05\%$). The conductance of the adjusted stock solution agreed with the value interpolated from the data of Stokes[10]. Using density values from ref. 11, other solutions were obtained by weight dilution of the stock.

Solutions of DCl in D_2O were prepared using the same procedure. The D_2O (deuterium content > 99.99 atom %, IC-Chemikalien, München) had a specific conductance of $<2\times10^{-6}\ \mathrm{S\ cm^{-1}}$, and was used without further purification. DCl was obtained as a 36 wt% solution in D_2O (D content > 99.9%). We used the density of pure D_2O given in ref. 12, and assumed the partial molar volume of HCl to be the same in H_2O and D_2O, which allowed us to convert from weight per cent to molarity. This assumption was verified by some representative density measurements with an Anton Paar vibrating-tube densimeter (accuracy, $\pm2\times10^{-5}\ \mathrm{g\ cm^{-3}}$).

Mixed solutions of the desired deuterium content (D atom fractions $X_D=0.25$, 0.5 and 0.75) were prepared by mixing HCl-H_2O solutions with DCl-D_2O solutions of the same molarity. The same procedure was applied for obtaining solutions of KCl in H_2O-D_2O mixtures. The small excess volume of mixing

‡ Correspondence can be addressed to either author.